



Reduction and pH Dual-Responsive Block Copolymers Containing Pendent *p*-Nitrobenzyl Carbamate Functionalities: Synthesis and Self-Assembly Behavior

Cong Hu, Bingyang Dong, Li Liu

Key Laboratory of Functional Polymer Materials, Ministry of Education, Institute of Polymer Chemistry, College of Chemistry, Nankai University, Tianjin 300071, People's Republic of China

Correspondence to: L. Liu (E-mail: nkliuli@nankai.edu.cn)

Received 27 February 2019; Revised 22 April 2019; accepted 22 April 2019

DOI: 10.1002/pola.29394

ABSTRACT: We report on the preparation of reduction-responsive amphiphilic block copolymers containing pendent *p*-nitrobenzyl carbamate (*p*NBC)-caged primary amine moieties by reversible addition–fragmentation chain transfer (RAFT) radical polymerization using a poly(ethylene glycol)-based macro-RAFT agent. The block copolymers self-assembled to form micelles or vesicles in water, depending on the length of hydrophobic block. Triggered by a chemical reductant, sodium dithionite, the *p*NBC moieties decomposed through a cascade 1,6-elimination and decarboxylation reactions to liberate primary amine groups of the linkages, resulting in the disruption of the assemblies. The reduction sensitivity of assemblies was affected by the length of hydrophobic block and the structure of amino acid-derived linkers. Using hydrophobic dye Nile red (NR) as a

model drug, the polymeric assemblies were used as nanocarriers to evaluate the potential for drug delivery. The NR-loaded nanoparticles demonstrated a reduction-triggered release profile. Moreover, the liberation of amine groups converted the reduction-responsive polymer into a pH-sensitive polymer with which an accelerated release of NR was observed by simultaneous application of reduction and pH triggers. It is expected that these reduction-responsive block copolymers can offer a new platform for intracellular drug delivery. © 2019 Wiley Periodicals, Inc. *J. Polym. Sci., Part A: Polym. Chem.* 2019

KEYWORDS: block copolymers; micelles; reduction; self-assembly; stimuli-sensitive polymers

INTRODUCTION Stimuli-responsive polymers that can change their properties in response to either exogenous or endogenous stimuli have played important roles in the construction of diverse functional materials.^{1,2} To date, pH, temperature, and glutathione (GSH)-based stimuli-responsive polymeric assemblies have been extensively developed in drug delivery.^{3–5} However, these carriers were proven unsatisfactory *in vivo* because of their lack of sensitivity to respond at the early stage of tumor development. It is reported that hypoxia contributes to cancer progression by assisting in the activation of cell signaling pathways that regulate angiogenesis and apoptosis.⁶ Hypoxia, deficient oxygen supply in tissues, is a significant hallmark of various intractable diseases, including tumor,^{7,8} stroke,⁹ vascular ischemia,¹⁰ and inflammatory disease.^{11,12} Jiang and coworkers¹³ reported a hypoxia-specific macromolecular probe which could detect cancer cells at a very early stage of tumor development and lymph node metastasis. It is appealing to develop functional polymers responsive to hypoxic microenvironment for the treatment of hypoxia-associated diseases.

Since tumor hypoxia leads to elevated levels of some reductive enzymes, such as nitroreductase (NTR), degenerative transfer

(DT)-diaphorase, and azoreductase,^{14–16} the reduction-responsive polymers under hypoxic environment provide an important strategy for selective tumor targeting. Nitroimidazoles, nitroaromatic, and azoaromatic and quinone compounds are three representative classes of hypoxia-responsive moieties and useful for the design of prodrugs,^{17–19} fluorescent probes,^{20–22} and nanocarriers.²³ For example, the reducible azobenzene units were introduced into the polymers as pendent groups or a linker, and azobenzene imparted hypoxia sensitivity and specificity of the polymers.²⁴ Based on the polymers containing azobenzene units as cleavable linkers, Khan and coworkers fabricated enzyme-responsive assemblies,^{25,26} and developed copolymers capable of transforming into polycations through a cascade self-immolative process.^{27–29} As the azobenzene units were reduced to the corresponding anilines by azoreductase under the hypoxic condition, the polymeric assemblies formed by azobenzene-containing polymers successfully released the encapsulated drugs or siRNA to hypoxic cancer cells.^{30,31} It was found that doxorubicin (DOX)-loaded nanoparticles of nitroimidazole-modified polymers selectively accumulated at the hypoxic tumor tissues and exhibited high antitumor activity *in vivo*.³²

Additional supporting information may be found in the online version of this article.

© 2019 Wiley Periodicals, Inc.

Under hypoxic conditions, *p*-nitrobenzyl alcohol derivatives (NADs) are highly labile and readily degraded by a 1,6-elimination reaction in the presence of NTR with nicotinamide adenine dinucleotide as an electron donor.³³ Therefore, NADs have been widely used to design prodrugs^{34–37} and fluorescent sensors^{38,39} for NTR and hypoxia. However, reduction-responsive polymers based on NADs are less exploited. Park and coworkers⁴⁰ prepared an amphiphilic block copolymer by the conjugation of the hydrophobic NADs to the side chains of poly (ethylene glycol) (PEG)-*b*-polylysine, and found that the DOX-loaded copolymer micelles exhibited rapid intracellular release of DOX under hypoxic conditions. Jo and coworkers⁴¹ synthesized a biodegradable polyurethane based on a monomer containing NAD, and further prepared paclitaxel-loaded nanoparticles. In the presence of a chemical reductant, sodium dithionite (Na₂S₂O₄), the reduction of pendent aryl nitro group to amine initiated a cascade of self-immolative processes, ultimately leading to systemic degradation of the polymer and a rapid release of encapsulated paclitaxel.

Polymers possessing protonable amine functionalities are attractive building blocks for the fabrication of pH-responsive assemblies. Arme's group and Liu's group prepared various block copolymers based on amine-containing monomers and investigated their self-assembly behaviors induced by the protonation of amine moieties.^{42–46} In recent years, taking advantage of selectively decaging of carbamate and the release of amine on demand, Liu's group synthesized a series of amphiphilic block polymers possessing pendent carbamate-masked amine moieties and constructed stimuli-responsive polymersomes with responsiveness toward oxidation,^{47,48} enzyme,⁴⁹ and light.⁵⁰

Herein, we prepare well-defined reduction-responsive amphiphilic diblock copolymers via reversible addition–fragmentation chain transfer (RAFT) polymerization of methacrylate (MA) monomer modified with *p*-nitrobenzyl carbamate (*p*NBC) moiety via an amino acid-derived linker from L-phenylalanine or L-valine. Depending on the hydrophobic block length, the diblock copolymers self-assemble into spherical micelles or vesicles in water. The diblock copolymers are expected to detach the pendent *p*NBC moieties once the aryl nitro groups reduce into the corresponding amine, which can spontaneously initiate a cascade 1,6-elimination and decarboxylation reactions to liberate the primary amine groups of the linkers. The unmasked primary amine groups turn the diblock copolymer more hydrophilic and pH responsive. Na₂S₂O₄, a bioorthogonal reducing agent mimic of some reductive enzymes such as NTR, DT diaphorase, and azoreductase, is utilized as a chemical reductant to investigate the reduction-responsive property of the polymeric self-assemblies. Under a simulated redox stress with Na₂S₂O₄, the decomposition of *p*NBC moieties results in the disruption of the polymeric self-assemblies. The reduction sensitivity of the assemblies is affected by the structure of amino acid-derived linker and the length of hydrophobic block. Using hydrophobic dye Nile red (NR) as a model drug, the release behavior of NR from the NR-loaded nanoparticles is studied in response to a simulated redox stress under different pHs. The incorporation of the reduction triggers, *p*NBC moieties, and amino acid-derived linkers endows the NR-loaded nanoparticles with reduction and pH dual-responsive release behavior.

EXPERIMENTAL

Materials

PEG monomethyl ether (mPEG₄₅-OH, *M_n* 2000, 98%) was purchased from Tokyo Chemical Industry (TCI). 2-Hydroxyethyl methacrylate (HEMA, 98%) was obtained from Heowns, Tianjin, China. HEMA was purified by washing an aqueous solution of HEMA with hexanes to remove ethylene glycol dimethacrylate, salting the monomer out of the aqueous phase with sodium chloride, drying over MgSO₄, and distilling under reduced pressure. 4,4'-Azobis(4-cyanopentanoic acid) (ACPA, 97%; Sigma-Aldrich, Shanghai, China) was recrystallized twice from methanol. L-Phenylalanine (L-Phe-OH, 99%; Heowns), L-valine (L-Val-OH, 99%; Aladdin, 99%), (4-cyanopentanoic acid) dithiobenzoate (CPADB; Aladdin, Shanghai, China), dimethylaminopyridine (DMAP, 99%; J&K Scientific Ltd., Beijing, China), dicyclohexylcarbodiimide (DCC; Sigma-Aldrich, 99%), Na₂S₂O₄ (97%; Dingguo Bio-Technology Co., Ltd., Beijing, China), 4-nitrobenzyl chloroformate (97%; Energy Chemical, Shanghai, China), and NR (99%; J&K Scientific Ltd.) were commercial products and used as received. All solvents were redistilled before use.

Characterizations

Nuclear magnetic resonance (¹H NMR) spectra were recorded on a Bruker 400 MHz NMR spectrometer using CD₃OD, CDCl₃, or *d*₆-dimethyl sulfoxide (DMSO) as the solvent. The number-average molecular weights (*M_n*), weight-average molecular weights (*M_w*), and polydispersities (*M_w*/*M_n*) of the polymers were determined by gel permeation chromatography (GPC) at 35 °C with a Waters 1525 chromatograph equipped with a Waters 2414 refractive index detector. Tetrahydrofuran (THF) was used as the eluent at a flow rate of 1 mL min⁻¹, and polystyrene standards were used for calibration. Matrix-assisted laser desorption ionization time of flight mass spectrometry (MALDI TOF MS) was carried out on AutoflexIII LRF200-CID. Ultraviolet–visible (UV–vis) spectroscopy was performed on a Shimadzu UV-2450 UV–vis spectrophotometer (Shimadzu (China) Co., LTD., Beijing). Fluorescence spectroscopy was measured on an RF-5301(Shimadzu) fluorospectrometer. Static laser scattering measurements were performed on a laser light scattering spectrometer (BI-200SM) equipped with a digital correlator (BI-9000AT) at 532 nm. Dynamic light scattering (DLS) analysis was conducted on a Zetasizer Nano ZS from Malvern Instruments (Malvern, United Kingdom) equipped with a 10 mW He–Ne laser at a wavelength of 633 nm at a 90° angle. Zeta potential measurements were conducted on a Zetasizer Nano ZS from Malvern Instruments. Transmission electron microscopy (TEM) observations were carried out on a Tecnai G2 20 S-TWIN electron microscope equipped with a Model 794 CCD camera. The samples were deposited on a carbon-coated copper grid, and water was evaporated in air. To increase the contrast, the samples were stained with OsO₄ vapor.

Synthesis of Amino Acid Derivatives Consisting of *p*NBC Groups (*p*NBC-Amino Acids)

The derivatives of L-Phe-OH and L-Val-OH were synthesized according to a modification of a previously reported protocol.⁵¹ In

a typical procedure, a solution of *p*-nitrobenzyl chloroformate (7.2 mmol) in dioxane (15 mL) was added to a solution of L-Phe-OH (1 g, 6 mmol) in aqueous Na₂CO₃ (15 mL, 6 mmol) at 0 °C. The reaction proceeded for 10 h under stirring at room temperature. The solution was extracted with ethyl acetate (10 mL), and the aqueous phase was acidified with 1 M aqueous HCl until no further white precipitation was produced. The precipitation was dried in vacuum to give *p*NBC-Phe-OH as a white powder (1.3 g, 62%). ¹H NMR [Fig. S1 (Supporting Information), 400 MHz, CD₃OD]: δ = 8.19 (d, NO₂C₆H₄, 2H), 7.51 (d, NO₂C₆H₄, 2H), 7.42 (m, OCONHCH, 1H), 7.25 (m, C₆H₅, 5H), 5.16 (s, NO₂C₆H₄CH₂, 2H), 4.44 (m, COCHNH, 1H), 3.22 and 2.95 ppm (m, C₆H₅CH₂CH, 2H). TOF MS (MALDI): calcd. for [M(C₁₇H₁₆N₂O₆) + Na]⁺: *m/z* = 367.10; found: 367.14.

Similarly, *p*NBC-Val-OH was synthesized by the reaction of L-Val-OH and *p*-nitrobenzyl chloroformate (yield: 71%). ¹H NMR [Fig. S2 (Supporting Information), 400 MHz, CD₃OD]: δ = 8.25 (d, NO₂C₆H₄, 2H), 7.61 (d, NO₂C₆H₄, 2H), 7.37 (m, OCONHCH, 1H), 5.23 (m, NO₂C₆H₄CH₂, 2H), 4.10 (d, COCHNH, 1H), 2.19 (m, (CH₃)₂CH, 1H), 0.99 ppm (m, (CH₃)₂CH, 6H). TOF MS (MALDI): calcd. for [M(C₁₃H₁₆N₂O₆) + Na]⁺: *m/z* = 319.10; found: 319.08.

Synthesis of *p*NBC-Modified MA

The *p*NBC-modified MAs (*p*NBC-AA-MA) were synthesized by esterification of HEMA and *p*NBC-amino acids according to a literature.⁵² In a typical procedure, *p*NBC-Phe-OH (0.9 g, 3 mmol) and HEMA (0.3 g, 2.5 mmol) were dissolved in dry THF (15 mL) under Ar atmosphere. A solution of DCC (0.66 g, 3.75 mmol) and DMAP (56 mg, 0.5 mmol) in dry THF (15 mL) was added dropwise to the solution under stirring at 0 °C, and the reaction was allowed to proceed for 1 h at 0 °C and for 24 h at room temperature. After the insoluble *N,N'*-dicyclohexylurea was filtrated, the filtrates were concentrated, and then dissolved in dichloromethane (DCM). The solution was washed with saturated NaHCO₃ and brine solution, and dried over anhydrous Na₂SO₄. After the solvent was removed by rotary evaporation, the crude product was purified by silica gel column chromatography using hexane/ethyl acetate/DCM (8:2:1, v/v/v) as the mobile phase to get a white solid compound *p*NBC-Phe-HEMA (0.78 g, 74%). ¹H NMR [Fig. S3 (Supporting Information), 400 MHz, CDCl₃]: δ = 8.19 (d, NO₂C₆H₄, 2H), 7.44 (d, NO₂C₆H₄, 2H), 7.28–7.10 (m, C₆H₅, 5H), 6.12 and 5.59 (s, C=CH₂, 2H), 5.27 (d, OCONHCH, 1H), 5.18 (m, NO₂C₆H₄CH₂, 2H), 4.68 (m, COCHNH, 1H), 4.49–4.29 (m, OCH₂CH₂O, 4H), 3.25–3.02 (m, C₆H₅CH₂, 2H), 1.94 ppm (s, C=CCH₃, 3H). TOF MS (MALDI): calcd. for [M(C₂₃H₂₄N₂O₈) + Na]⁺: *m/z* = 479.15; found: 479.16.

Similarly, *p*NBC-Val-HEMA was prepared from HEMA and *p*NBC-Val-OH (yield: 93%). ¹H NMR [Fig. S4 (Supporting Information), 400 MHz, CDCl₃]: δ = 8.22 (d, NO₂C₆H₄, 2H), 7.52 (d, NO₂C₆H₄, 2H), 6.12 and 5.59 (s, C=CH₂, 2H), 5.33 (s, OCONHCH, 1H), 5.20 (s, NO₂C₆H₄CH₂, 2H), 4.52–4.28 (m, OCH₂CH₂O and COCHNH, 5H), 2.18 (m, (CH₃)₂CH, 1H), 1.94 (s, C=CCH₃, 3H), 0.99 [m, (CH₃)₂CH, 6H]. TOF MS (MALDI): calcd. for [M(C₁₉H₂₄N₂O₈) + Na]⁺: *m/z* = 431.15; found: 431.

Synthesis of mPEG₄₅-CPADB Macro-RAFT Agent

PEG-based macro-RAFT agent was prepared by the esterification of mPEG₄₅-OH and CPADB in the presence of DCC and DMAP.⁵³ In a typical procedure, mPEG₄₅-OH (1 g, 0.5 mmol) was dissolved in anhydrous toluene (10 mL), and then azeotropic distillation was carried out to remove most of the solvent. CPADB (0.3 g, 1 mmol) and dry DCM (20 mL) were added. After cooling to 0 °C, DCC (0.23 g, 1 mmol) and DMAP (12 mg, 0.1 mmol) in DCM (20 mL) was added dropwise over 1 h. The reaction mixture was stirred at room temperature for 24 h. After removing insoluble salts by filtration, the filtrates were concentrated, and then precipitated into an excess of cold diethyl ether. The dissolution-precipitation cycle was repeated twice. The mPEG₄₅-CPADB macro-RAFT agent was dried overnight under vacuum at room temperature and obtained as a red powder (1 g, 88%). ¹H NMR (400 MHz, CDCl₃): δ = 7.89 (d, C₆H₅, 2H), 7.56 (t, C₆H₅, 1H), 7.42 (t, C₆H₅, 2H), 4.27 (t, COOCH₂, 2H), 3.83–3.46 (m, OCH₂CH₂O, 202H), 3.38 (m, CH₃O, 3H), 2.72–2.23 (m, CH₂CH₂COO, 4 H), 1.93 [m, SC(CN)CH₃, 3H].

Synthesis of mPEG₄₅-*b*-P(*p*NBC-AA-MA) Block Copolymers by RAFT Polymerization

A typical procedure to synthesize the block copolymer from mPEG₄₅-CPADB macro-RAFT agent was described as follows. *p*NBC-Phe-HEMA (0.2 g, 0.44 mmol), mPEG₄₅-CPADB (0.01 g, 0.044 mmol), and ACPA (3.07 mg, 0.01 mmol) were dissolved in DMF (1.6 mL) in a flask. The flask was degassed by three freeze-pump-thaw cycles. The block copolymerization was carried out at 80 °C for 24 h. The polymerization was stopped by cooling the solution in ice water and exposing to air. The reaction solution was concentrated, and then CH₂Cl₂ was added. The block polymer, mPEG₄₅-*b*-P(*p*NBC-Phe-HEMA)_n, was precipitated into an excess of cold ethanol, centrifuged, and dried overnight under vacuum at room temperature.

Preparation of Block Copolymer Assemblies

Typically, 10.0 mg of a block copolymer was dissolved in 2 mL of THF, and deionized water (6 mL) was added dropwise into the solution under stirring within 30 min. The solution was transferred to a dialysis bag [molecular weight cutoff (MWCO) = 12 kDa], and dialyzed against deionized water for 48 h. The deionized water was replaced every 4 h.

Measurement of Critical Aggregation Concentration by Fluorescence Spectroscopy

Pyrene was used as a fluorescence probe to determine the critical aggregation concentration (CAC) of the block copolymers. A pre-determined amount of pyrene in acetone solution was added to volumetric flasks, and acetone was then evaporated completely. A series of the aqueous solutions of block polymer with different concentrations were added to the flasks, and the concentration of pyrene in each flask was fixed at 1.0 × 10⁻⁷ mol L⁻¹. The solution was in equilibrium for 30 min at room temperature. The excitation spectra of all solutions were recorded at 25 °C (λ_{em} = 390 nm). The intensity ratios at bands 333 and 338 nm (I₃₃₈/I₃₃₃) of all solutions were measured. The CAC was obtained from the intersection of two tangent plots of intensity ratio I₃₃₈/I₃₃₃ versus the logarithm of polymer concentration.

Reduction Responsiveness of Block Copolymer Assemblies

The reduction of the block copolymers was tested with a chemical reducing agent, $\text{Na}_2\text{S}_2\text{O}_4$. In brief, $\text{Na}_2\text{S}_2\text{O}_4$ (50-fold molar excess to the number of *p*-nitrobenzyl group) was added to the aqueous solution of block copolymer assemblies (1 mg mL^{-1}) at pH 6.0 and 7.4, respectively. The solution was stirred at 37°C , and the samples were taken at specified intervals and analyzed by UV-vis and DLS. After 24 h, the solution was dialyzed against the deionized water for 2 days. The reduced block copolymer was recovered by lyophilization and characterized by ^1H NMR.

Preparation of NR-Loaded Nanoparticles

Typically, block copolymer (10 mg) and NR (0.1 mg) were dissolved in 2 mL of THF. Then, 6 mL of deionized water was added dropwise for 30 min under stirring. The solution was stirred for another 6 h at room temperature, and the organic solvent was removed by dialysis (MWCO = 12 kDa) against deionized water for 48 h in the dark to obtain the NR-loaded micelles.

Release of NR

The release of NR from block copolymer nanoparticles was studied at pH 7.4 (phosphate buffer solution, 50 mM) and 6.0 (acetate buffer solution, 50 mM), respectively. In a typical experiment, $\text{Na}_2\text{S}_2\text{O}_4$ (50-fold molar excess to the number of *p*-nitrobenzyl group) was added to the solution of NR-loaded nanoparticles, and the solution was stirred at 37°C . A fluorescence spectrophotometer was used to monitor the release of NR from the nanoparticles with time. Fluorescence emission spectra were recorded at $\lambda_{\text{ex}} = 550 \text{ nm}$. As a control, the release of NR without $\text{Na}_2\text{S}_2\text{O}_4$ was also monitored under the same conditions.

RESULTS AND DISCUSSION

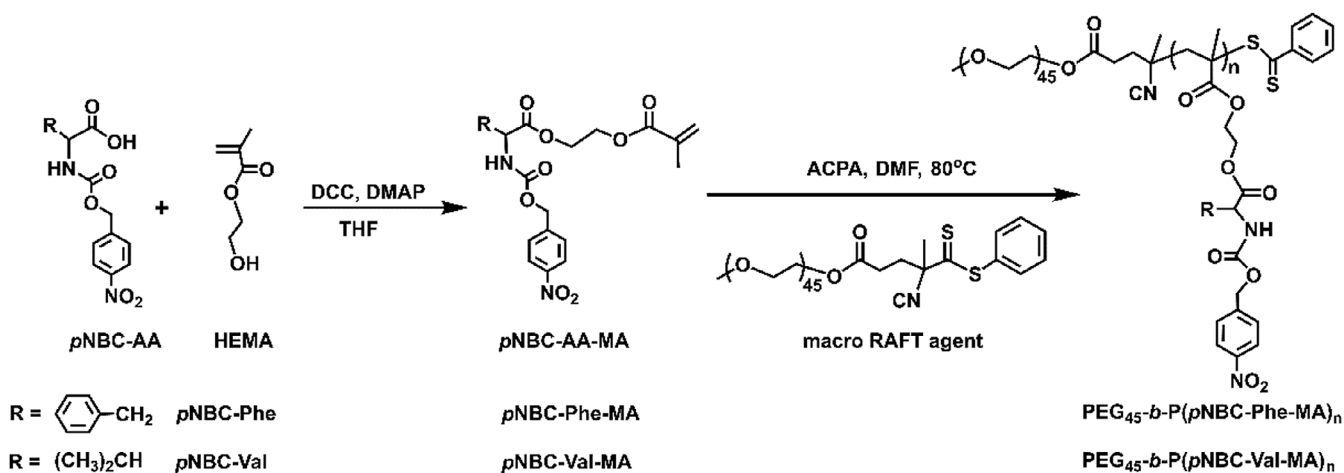
Synthesis of Block Copolymers Containing Pendant *p*-Nitrobenzyl Carbamate Triggers

Many designs for fluorescent probes⁵⁴ and bioreductive drugs^{18,55} have explored *p*-nitrobenzyl carbamates (*p*NBCs) as triggers, which can act as a substrate for mitochondrial NTR-mediated reduction

in hypoxic tumor. NTR reduces nitroaromatic moiety in *p*NBC to electron-donating hydroxylamine or amine species, followed by a cascade 1,6-elimination and decarboxylation reactions, and simultaneous release of amine-based effector. In this article, reduction-responsive block copolymers were prepared by direct RAFT polymerization of methacrylate (MA) modified with *p*NBC moiety via an amino acid-derived linker from *L*-phenylalanine or *L*-valine. We started with the synthesis of *p*NBC-caged amino acids (*p*NBC-AA) by the coupling reaction of *p*-nitrobenzyl chloroformate with *L*-Phe-OH and *L*-Val-OH, respectively, and then performed the esterification reactions of HEMA and *p*NBC-AAs to yield MA monomers, *p*NBC-Phe-MA, and *p*NBC-Val-MA, containing carbamate functionality and reduction-active capping trigger. The chemical structures of *p*NBC-Phe-MA and *p*NBC-Val-MA were confirmed by ^1H NMR and MS analyses. The RAFT polymerization of *p*NBC-Phe-MA or *p*NBC-Val-MA was carried out in DMF at 80°C using PEG₄₅-based macro-RAFT agent, affording amphiphilic diblock copolymers PEG₄₅-*b*-P(*p*NBC-Phe-MA)_{*n*} and PEG₄₅-*b*-P(*p*NBC-Val-MA)_{*n*} (Scheme 1). These diblock copolymers displayed unimodal molecular weight and narrow polydispersities (Fig. 1). ^1H NMR spectroscopy was used to characterize the chemical structures of PEG₄₅-*b*-P(*p*NBC-Phe-MA)_{*n*} and PEG₄₅-*b*-P(*p*NBC-Val-MA)_{*n*} (Fig. 2). The signals corresponding to *p*-nitrobenzyl moieties appear at δ 8.14 (Peak a), 7.58 (Peak b), and 5.02 ppm (Peak c), and the characteristic signals of PEG are observed at δ 3.3 (CH₃O) and 3.5 ppm (OCH₂CH₂O). The number-average polymerization degree (DP_n) of NBC-AA-MA units was calculated by the integration ratio of PEG signals at δ 3.5 ppm (Peaks j, k, and l) and methylene groups (Peak c, δ 5.02 ppm) in the *p*NBC-AA-MA units. A series of PEG₄₅-*b*-P(*p*NBC-Phe-MA)_{*n*} and PEG₄₅-*b*-P(*p*NBC-Val-MA)_{*n*} block copolymers with various hydrophobic block lengths were readily prepared by tuning the feeding ratios of monomer to macro-RAFT agent. The structural parameters of these block copolymers are summarized in Table 1.

Self-Assembly Behavior in Aqueous Solution

The obtained PEG₄₅-*b*-P(*p*NBC-Phe-MA)_{*n*} and PEG₄₅-*b*-P(*p*NBC-Val-MA)_{*n*} diblock copolymers are expected to self-assemble in the aqueous solution due to their amphiphilic nature. Using pyrene as a



SCHEME 1 Synthetic routes for the preparation of *p*NBC-AA-MA monomers and reduction-responsive PEG₄₅-*b*-P(*p*NBC-AA-MA)_{*n*} diblock copolymers.

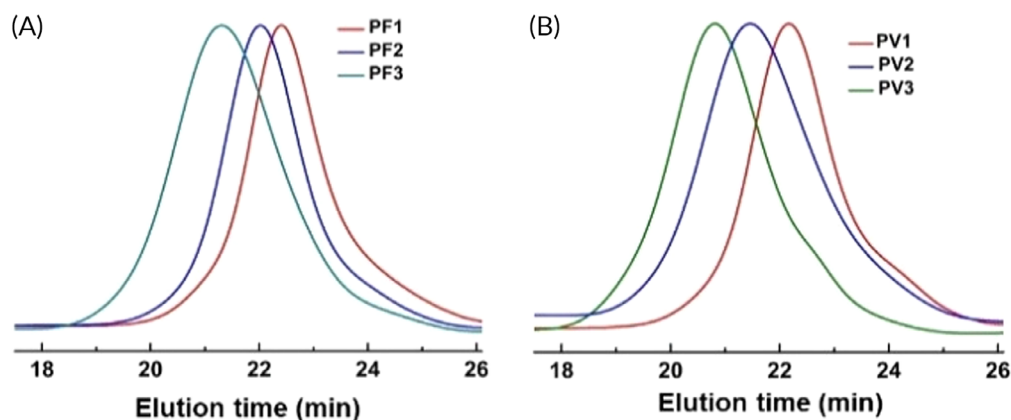


FIGURE 1 GPC traces of (A) PEG₄₅-*b*-P(*p*NBC-Phe-MA)_{*n*} and (B) PEG₄₅-*b*-P(*p*NBC-Val-MA)_{*n*} block copolymers. [Color figure can be viewed at wileyonlinelibrary.com]

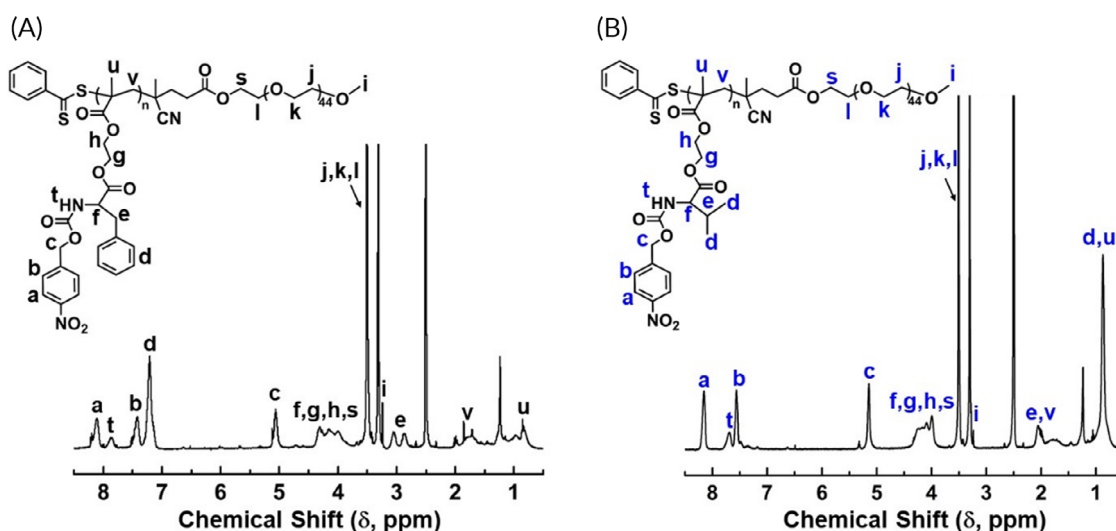


FIGURE 2 ¹H NMR spectra of block copolymer PF1 (A) and block copolymer PV1 (B) in *d*₆-DMSO. [Color figure can be viewed at wileyonlinelibrary.com]

hydrophobic fluorescence probe, the fluorescence spectroscopy was utilized to investigate the formation of self-assemblies from PEG₄₅-*b*-P(*p*NBC-Phe-MA)_{*n*} and PEG₄₅-*b*-P(*p*NBC-Val-MA)_{*n*} in the aqueous solution. It was reported that the concentration dependence of the I_{338}/I_{333} ratios of the (0, 0) band of pyrene was very sensitive to CAC.⁵⁶ The intensity ratio of I_{338}/I_{333} was plotted against the concentration of the block copolymers. As shown in

Figure 3, the I_{338}/I_{333} ratio remained almost constant at low concentrations, and increased sharply once the copolymer concentration reached the CAC, indicating the formation of self-assemblies and the encapsulation of pyrene in the hydrophobic environment. From the sigmoidal shape curves, the CAC values were determined and shown in Figure 3. As the length of P(*p*NBC-Phe-MA) block increases from 11 to 26, the CAC values of PEG₄₅-*b*-P(*p*NBC-Phe-MA)_{*n*} block

TABLE 1 Block Copolymerization of *p*NBC-AA-MA with mPEG₄₅-CPADB Macro-RAFT Agent

Entry	Block Copolymer	[M]/[CTA]/[I] (mol mol ⁻¹ mol ⁻¹)	DP _{n,NMR} ^a	M _{n,GPC} ^b (kDa)	PDI ^b
PF1	PEG ₄₅ - <i>b</i> -P(<i>p</i> NBC-Phe-MA) ₁₁	40/4/1	11	6.5	1.13
PF2	PEG ₄₅ - <i>b</i> -P(<i>p</i> NBC-Phe-MA) ₁₇	80/4/1	17	7.5	1.15
PF3	PEG ₄₅ - <i>b</i> -P(<i>p</i> NBC-Phe-MA) ₃₁	120/4/1	31	9.6	1.19
PV1	PEG ₄₅ - <i>b</i> -P(<i>p</i> NBC-Val-MA) ₁₃	40/4/1	13	7.0	1.13
PV2	PEG ₄₅ - <i>b</i> -P(<i>p</i> NBC-Val-MA) ₁₉	90/4/1	19	9.1	1.25
PV3	PEG ₄₅ - <i>b</i> -P(<i>p</i> NBC-Val-MA) ₂₆	120/4/1	26	11.6	1.21

^a Calculated by ¹H NMR.

^b Determined by GPC using THF as the eluent.

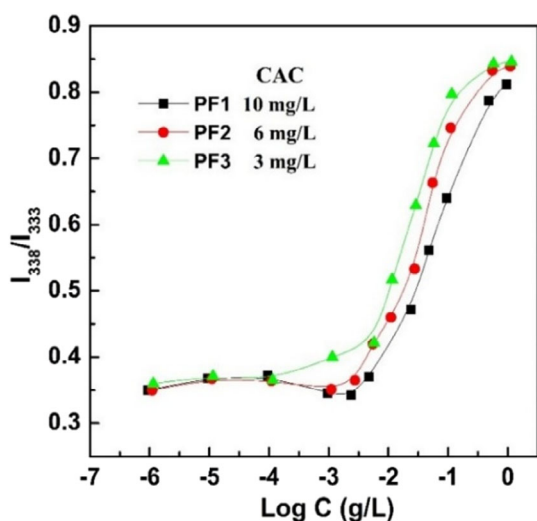


FIGURE 3 Dependence of the intensity ratio I_{338}/I_{333} from excitation spectra of pyrene on the concentrations of PF1, PF2, and PF3 block copolymers ($\lambda_{em} = 390$ nm). [Color figure can be viewed at wileyonlinelibrary.com]

copolymers change from 10 to 3 mg L⁻¹. For PV1–PV3 block copolymers, the CAC values decrease from 28 to 18 mg L⁻¹ with the

increasing of hydrophobic block length (Fig. S5, Supporting Information). It is also noted that the CAC values of PV block copolymers are higher than those of PF block copolymers with similar hydrophobic block length, which is ascribed to the high hydrophobicity of phenyl groups and the π - π stacking interactions between phenyl rings.^{51,57}

The hydrodynamic size of the self-assemblies was analyzed by DLS. Figure 4(A) compares the squared electric field correlation functions, $g_1^2(t)$, versus time, where the mean decay time is related to the average size of the self-assemblies. It is found that the self-assembled nanoparticles relaxed gradually slow with the increasing of hydrophobic block length, indicating the average size of assemblies became larger and larger. The DLS curves revealed the average hydrodynamic diameters, $\langle Dh \rangle$, of the PF1, PF2, and PF3 copolymer assemblies were 70, 120, and 170 nm [Fig. 4(B)], respectively. TEM images demonstrate PF1 and PF2 copolymers self-assembled into micellar nanoparticles in the aqueous media [Fig. 4(C,D)]. For PF3 copolymer, a vesicle structure is observed [Fig. 4(E)]. Moreover, static lighting scattering measurement revealed that the ratio ($\langle Rg \rangle / \langle Rh \rangle$) of mean square radius of gyration, $\langle Rg \rangle$, and hydrodynamic radius, $\langle Rh \rangle$, was close to 1 for PF3 copolymer, further confirming the formation of hollow structures. The formation of vesicles can be attributed to the longer hydrophobic block of PF3 copolymer that leads to the increased packing parameter as compared to those of PF1 and PF2.⁵⁸ For PV1–PV3 block

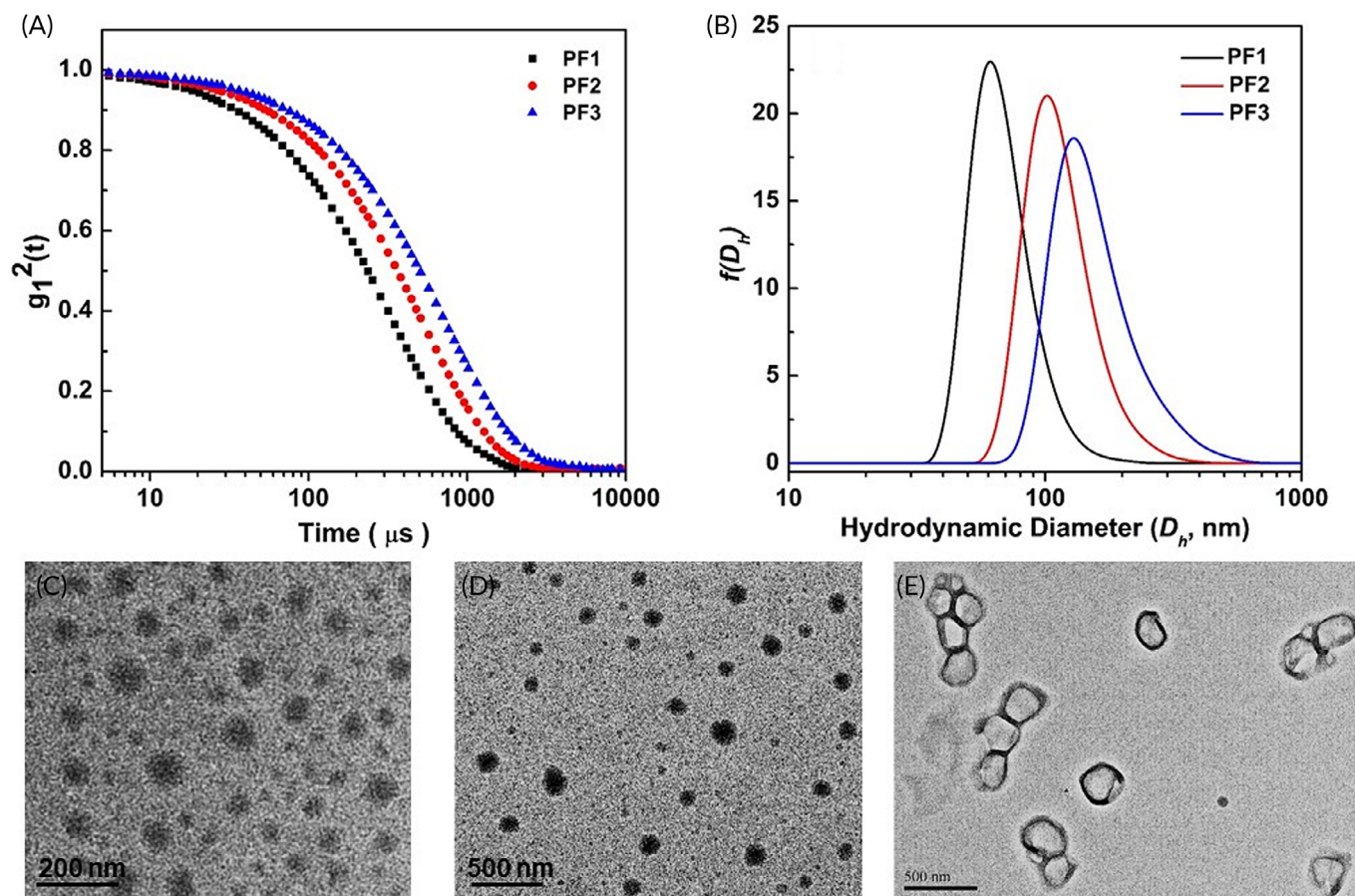


FIGURE 4 (A) Correlation functions, (B) DLS curves of self-assembled aggregates of PF1, PF2, and PF3, and (C–E) TEM images of self-assembled aggregates of PF1 (C), PF2 (D), and PF3 (E). [Color figure can be viewed at wileyonlinelibrary.com]

copolymers, DLS results also demonstrated the size of the assemblies increased with the hydrophobic block length. The $\langle Dh \rangle$ of the self-assemblies formed by PV1, PV2, and PV3 were 80, 180, and 280 nm, respectively (Fig. S6, Supporting Information). A similar self-assembly morphology was observed by TEM. PV1 and PV2 copolymers formed micellar nanoparticles, while PV3 with longer hydrophobic block self-assembled into vesicles.

Reduction Responsiveness of Assemblies

Since these block copolymers contain pendent *p*NBC capping moieties, the assemblies are expected to be reduction responsive. Taking PF1 micelles as a prototype, we studied the reactivity of PF1 micelles toward a chemical reductant, $\text{Na}_2\text{S}_2\text{O}_4$. The reaction was monitored by UV-vis spectroscopy. In the presence of $\text{Na}_2\text{S}_2\text{O}_4$, the characteristic absorbance peak of *p*NBC moieties centered at $\lambda_{275} \text{ nm}^{40}$ progressively decreased with time (Fig. S7, Supporting Information), which is ascribed to the decomposition of *p*NBC moieties upon reduction by $\text{Na}_2\text{S}_2\text{O}_4$. The reduction of aryl nitro to amine initiates a cascade 1,6-elimination and decarboxylation reactions to liberate primary amine groups of amino acid-derived linkers [Fig. 5(A)]. We also traced the reaction of PF2, PF3, and PV1–PV3 nanoparticles with $\text{Na}_2\text{S}_2\text{O}_4$ to investigate the effects of hydrophobic block length and linker structure on reduction sensitivity of the assemblies. Figure 5(B) shows the variation of absorbance at $\lambda_{275} \text{ nm}$ with time. It is found that the absorbance of PF1 micelles varies more quickly than other samples within 3 h, indicating PF1 micelles is more sensitive to the reduction. As the hydrophobic block length increases, both PF and PV assemblies become less sensitive to reduction as proven by a little change in the absorbance with time. For PV assemblies, the absorbance at $\lambda_{275} \text{ nm}$ changes more slowly than that of the assemblies formed

by the PF block copolymer with a similar length of hydrophobic block, implying the PV assemblies are less responsive to reduction than the PF assemblies.

With an increase in the hydrophobic block length, the assemblies become larger and larger, making $\text{Na}_2\text{S}_2\text{O}_4$ less accessible to the *p*NBC moieties in the hydrophobic domain of the assemblies. Therefore, the small assemblies formed by the block copolymer with short hydrophobic length are more sensitive to reduction. In the presence of $\text{Na}_2\text{S}_2\text{O}_4$, nitroaromatic moiety in *p*NBC is reduced to electron-donating hydroxylamine or amine species, followed by a cascade 1,6-elimination and decarboxylation reactions, and release of amine-based leaving group. Nucleofugacity governs the last step of self-immolation, that is, the release of a leaving group.⁵⁹ Due to the conjugation effect of phenyl group which can increase the nucleofugacity of the amine unit, the release rate of amine moieties in PF is faster than that in PV (Fig. S8, Supporting Information).

The solution of reduced PF1 micelles was dialyzed against H_2O after 24 h reaction with $\text{Na}_2\text{S}_2\text{O}_4$, and then fluorescamine (FA) was added to the purified solution. The emission spectrum of FA was recorded at $\lambda_{\text{ex}} = 390 \text{ nm}$. As shown in Figure 5(C), the mixture of PF1 micelles and FA was nonfluorescent; however, the mixture of the reduced PF1 micelles and FA displayed a strong emission at $\lambda_{480} \text{ nm}$, which was caused by amine-induced emission turn-on of FA.^{48,49} This result confirms the generation of free primary amine groups on block copolymer after reacting with $\text{Na}_2\text{S}_2\text{O}_4$.

We used ^1H NMR to analyze the structure of the reduced block copolymers. After 24 h reaction with $\text{Na}_2\text{S}_2\text{O}_4$, the reduced block polymers were recovered by lyophilization after thorough dialysis against water, and characterized by ^1H NMR. The ^1H NMR spectra

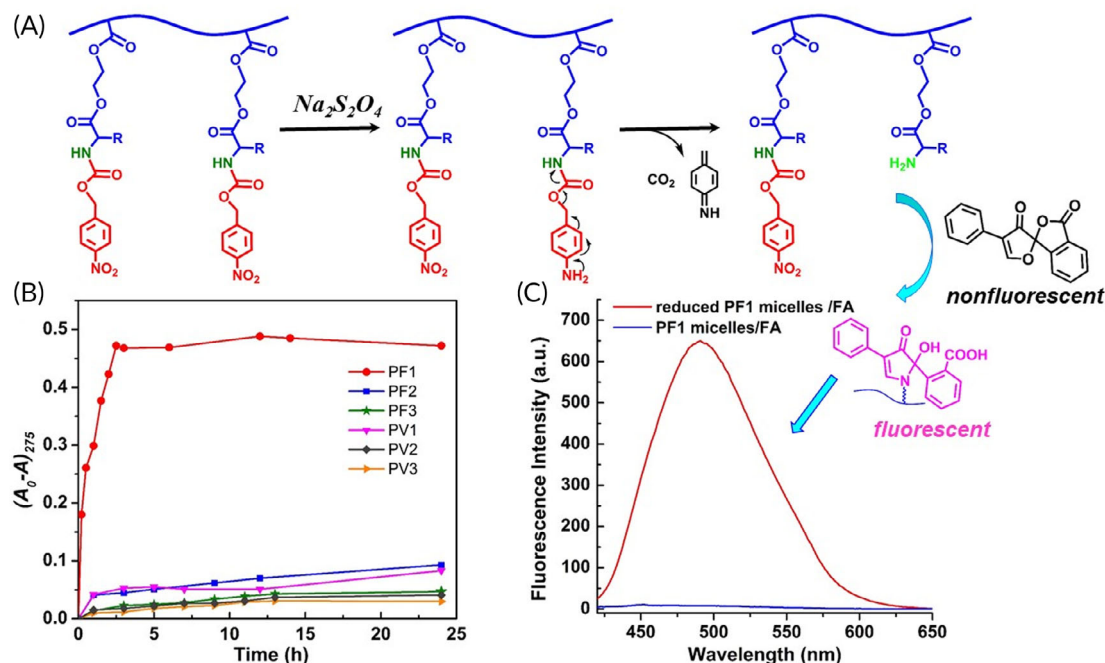


FIGURE 5 (A) The proposed mechanism showing reduction-responsive decomposition of block copolymer triggered by $\text{Na}_2\text{S}_2\text{O}_4$. (B) Variation of UV absorbance at $\lambda_{275} \text{ nm}$ of self-assemblies with time in the presence of $\text{Na}_2\text{S}_2\text{O}_4$ (37°C , pH 7.4). (C) Fluorescence analysis of original PF1 micelles and reduced PF1 micelles in the presence of FA ($\lambda_{\text{ex}} = 390 \text{ nm}$) [Color figure can be viewed at wileyonlinelibrary.com]

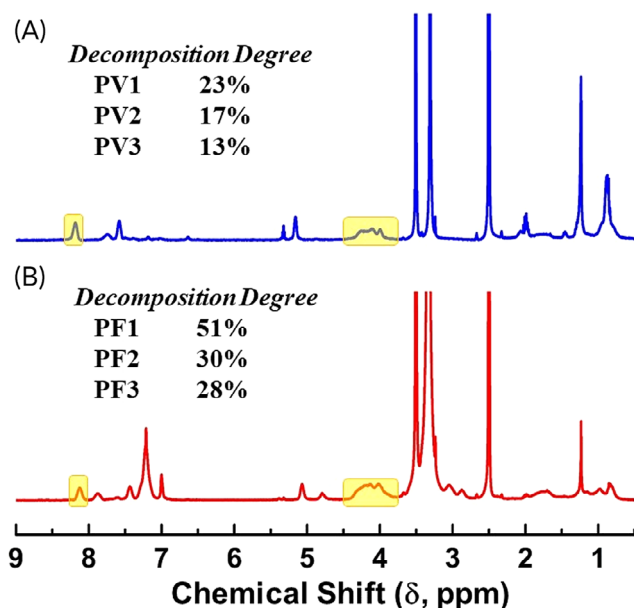


FIGURE 6 ^1H NMR spectra of reduced PF1 (A) and reduced PV1 (B) block copolymers in d_6 -DMSO. [Color figure can be viewed at wileyonlinelibrary.com]

of reduced PF1 and reduced PV1 block copolymers are shown in Figure 6. It is found that the intensities of the signals corresponding to *p*NBC moieties at δ 8.10, 7.50, and 5.09 ppm decreased, compared with ^1H NMR spectra shown in Figure 2. The decomposition degrees of various block copolymers were estimated based on the integration ratio of the signals at 4.0 ppm and the signal of *p*NBC moieties at 8.10 ppm. The data shown in Figure 6 reveal that half of *p*NBC moieties on PF1 are eliminated after 24 h reaction, and the nanoparticles are less sensitive to reduction with increasing the hydrophobic block length. For PV copolymers, less *p*NBC moieties decomposed in comparison with PF copolymers,

indicating that PV copolymers containing valine-derived linkers are more stable against reduction than PF copolymers.

We further traced the reduction-induced change in the hydrodynamic diameter of PF1 micelles by DLS. As shown in Figure 7, the micelles swelled rapidly within 30 min, and the $\langle D_h \rangle$ increased from 70 to 350 nm. Subsequently, the $\langle D_h \rangle$ progressively decreased from 350 to 40 nm within 2 h. It was also observed that the initial transparent solution became turbid within 30 min, and then slowly changed to transparent again after 2 h. In the presence of $\text{Na}_2\text{S}_2\text{O}_4$, the reduction of nitro group in *p*-nitrobenzyl to amine triggers the self-immolative decaging reaction to liberate primary amine group of the amino acid-derived linker (Scheme 2), which will increase the hydrophilicity of $\text{P}(p\text{NBC-Phe-MA})_{11}$ segment. The PF1 micelles swell as the hydrophobic block becomes a little hydrophilic due to the liberation of primary amine groups of the linkers. As more and more amine groups were liberated, the swollen micelles gradually dissociated into smaller micelles due to the increasing hydrophilicity. TEM image also revealed smaller micelles with a size of about 20–30 nm after 24 h reaction with $\text{Na}_2\text{S}_2\text{O}_4$, which agreed with the DLS result.

Reduction-Triggered Release of NR-Loaded Micelles

NR is a hydrophobic fluorescent probe whose quantum yield decreases with the increase in polarity of its microenvironment. To better understand the reduction profile of the block copolymer assemblies in aqueous solution, NR was encapsulated into PF (PF1–PF3) and PV (PV1–PV3) assemblies, and the fluorescence of the NR-loaded nanoparticle solutions was monitored against time. We investigated the release behaviors of NR from the nanoparticles in the buffer solutions at pH 7.4 (phosphate buffer solution) and 6.0 (acetate buffer solution), respectively (Fig. 8). There was no much difference in the release of NR under acidic and neutral conditions in the absence of $\text{Na}_2\text{S}_2\text{O}_4$, and the fluorescence intensity of

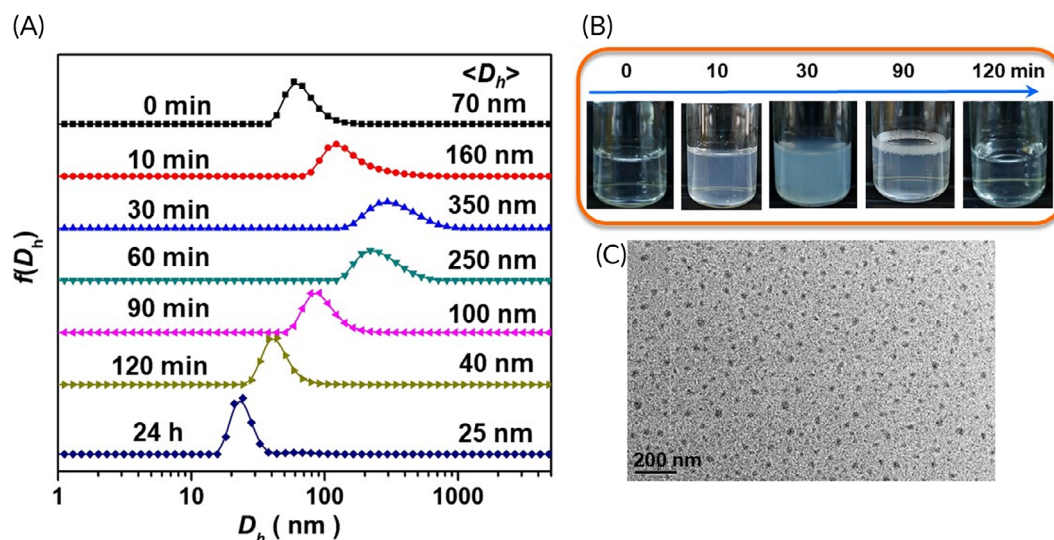
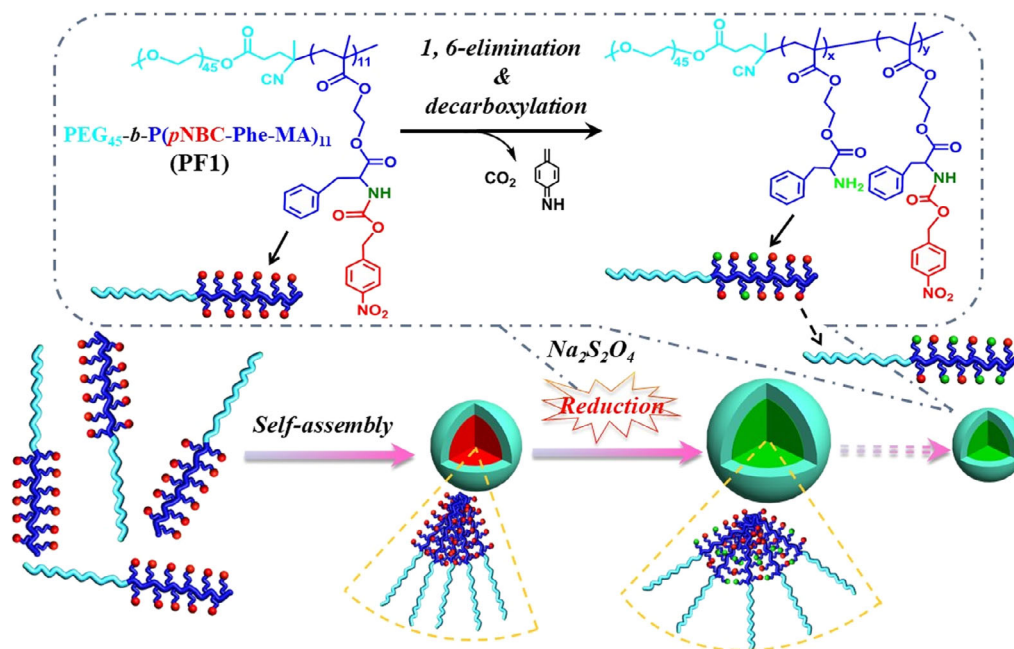


FIGURE 7 (A) DLS curves of PF1 micelles and (B) photos of PF1 micelle solution at specified intervals during the reaction with $\text{Na}_2\text{S}_2\text{O}_4$ at pH 7.4. (C) TEM images of the reduced PF1 micelles after 24 h reaction with $\text{Na}_2\text{S}_2\text{O}_4$. [Color figure can be viewed at wileyonlinelibrary.com]



SCHEME 2 Schematic illustration for the self-assembly of PF1 block copolymer into reduction-responsive micelles and response to a simulated redox stress. [Color figure can be viewed at wileyonlinelibrary.com]

NR decreased slightly with time, reaching more than 90% of the initial intensity after 4 h for all nanoparticles. Upon the addition of $\text{Na}_2\text{S}_2\text{O}_4$, the release of NR from all nanoparticles became faster, displaying a reduction-responsive profile. It is also found NR releases much more rapidly at pH 6.0 than at pH 7.4, thus demonstrating the incorporation of amino acid-derived linkers endows these block copolymer nanoparticles with pH-responsiveness upon reduction. For example, the fluorescence intensity of NR-loaded PF1 nanoparticle solution decreased to 72% of the initial intensity within 10 min at pH 7.4 in the presence of $\text{Na}_2\text{S}_2\text{O}_4$, and gradually decreased to 62% after 4 h. Furthermore, NR released from PF1 nanoparticles much more rapidly at pH 6.0, and the fluorescence intensity changed sharply to 30% of the initial intensity within

10 min and reached to 7% after 4 h. Since the reduction of *p*-nitrobenzyl triggered by $\text{Na}_2\text{S}_2\text{O}_4$ initiates the liberation of free amine groups of phenylalanine-derived linkers, the cores of NR-loaded PF1 nanoparticles become more and more hydrophilic as more and more amine groups protonate in acidic environment, resulting in accelerating the release of NR from the disrupted nanoparticles.

The UV-vis and ^1H NMR results indicate that PV assemblies are less responsive to reduction than PF assemblies, which is also confirmed by the release of NR. As shown in Figure 8, NR releases faster from PF nanoparticles than from PV nanoparticles formed by the PV block copolymer with a similar length of hydrophobic block. For example,

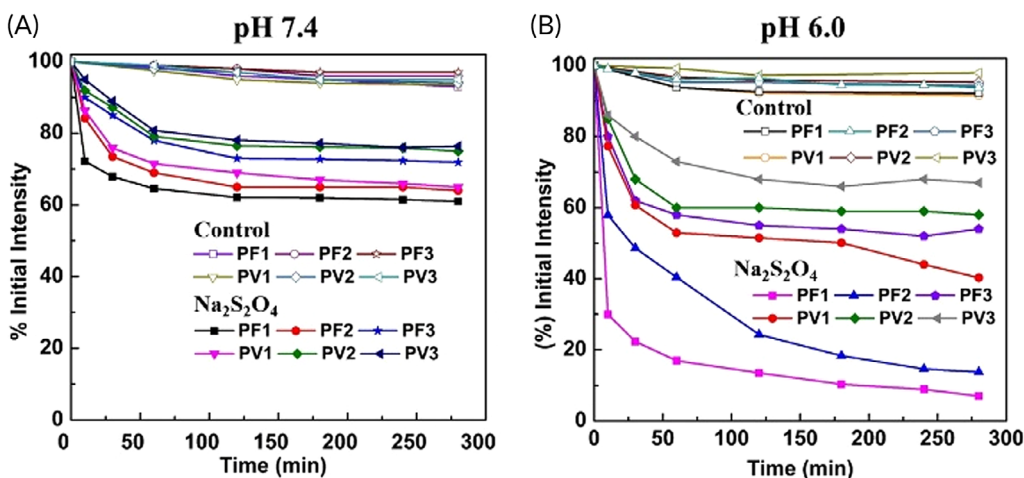


FIGURE 8 Time dependence of the relative emission intensity of NR fluorescence in PF and PV assemblies with or without $\text{Na}_2\text{S}_2\text{O}_4$ at (A) pH 7.4 and (B) pH 6.0. Copolymer concentration: 0.1 mg mL^{-1} ; NR concentration: $0.7 \text{ } \mu\text{g mL}^{-1}$; $37 \text{ } ^\circ\text{C}$. [Color figure can be viewed at wileyonlinelibrary.com]

only 14% of NR was released from PV1 nanoparticles within 10 min and 34% was released after 4 h at pH 7.4, while the PF1 nanoparticles released 28% of NR within 10 min and 38% after 4 h under the same conditions. This difference becomes pronounced at pH 6.0. PV1 nanoparticles released 23% of NR within 10 min and 56% after 4 h. For PF1 nanoparticles, approximately 70% of NR was released within 10 min and 91% was released after 4 h. The larger difference can be due to the increasing number of protonated amine groups of reduced PF1 at pH 6.0. As the hydrophobic block length of PF and PV copolymers increases, the release of NR from nanoparticles becomes slower due to the less reduction sensitivity of larger nanoparticles, which is in agreement with the results from the UV-vis studies. The decomposition of *p*NBC moieties leads to unmask the primary amine groups of the linkers, thus converting the reduction-responsive block copolymer to pH-responsive copolymer. The simultaneous application of reduction and pH stimuli induces a rapid disruption of nanoparticles. Therefore, the release of NR from these reduction-responsive block nanoparticles can be modulated by altering the structure of amino acid-derived linker, the length of stimuli-responsive polymer segment and the pH of milieu.

CONCLUSIONS

In summary, methacrylate monomers from *p*NBC-caged phenylalanine and valine were utilized to prepare amphiphilic block copolymers consisting of hydrophilic PEG block and hydrophobic block containing pendent reduction-trigger-capped amino acid-derived linkers. In the aqueous solution, the block copolymers self-assembled into spherical micelles and vesicles as the length of hydrophobic block increased. Upon reduced by a chemical reductant, $\text{Na}_2\text{S}_2\text{O}_4$, the *p*NBC moieties were decomposed through a cascade 1,6-elimination and decarboxylation reactions to liberate free primary amine groups of the linkers, resulting in the disruption of assemblies. The reduction rate of assemblies decreased as the hydrophobic block length became longer. It was also found that the assemblies of the block copolymers containing valine-derived linkers were less responsive to reduction, compared with those of the block copolymers containing phenylalanine-derived linkers. With NR as a model hydrophobic drug, the NR-loaded nanoparticles exhibited reduction-triggered release behavior in the presence of $\text{Na}_2\text{S}_2\text{O}_4$. Moreover, the decomposition of *p*NBC moieties also converted the reduction-responsive block copolymer into pH-responsive copolymer. Due to the protonation of the unmasked amines of the linkers under mildly acidic conditions, the release of NR was accelerated by simultaneous application of reduction and pH stimuli. Since the *p*NBC trigger can allow potential NTR-mediated reduction, the incorporation of *p*NBC moieties into polymers as the reduction-trigger will extend the redox-sensitive functionality from GSH-responsive disulfide to other biomolecule-responsive polymeric assemblies. Further investigation on the reduction responsiveness of these *p*NBC containing block copolymers in NTR and NADH tumor microenvironment is under way.

ACKNOWLEDGMENT

This project was financially supported by the National Natural Science Foundation of China under contract no. 51773100.

REFERENCES AND NOTES

- 1 M. C. Stuart, W. Huck, J. Genzer, M. Müller, C. Ober, M. Stamm, G. B. Sukhorukov, L. Szleifer, V. V. Tsukruk, M. Urban, F. Winnik, S. Zauscher, L. Luzinov, S. Minko, *Nat. Mater.* **2010**, *9*, 101.
- 2 Z. Ge, S. Liu, *Chem. Soc. Rev.* **2013**, *42*, 7289.
- 3 S. Mura, J. Nicolas, *Nat. Mater.* **2013**, *12*, 991.
- 4 E. Fleige, M. A. Quadir, R. Haag, *Adv. Drug Deliv. Rev.* **2012**, *64*, 866.
- 5 J. F. Quinn, M. R. Whittaker, T. P. Davis, *Polym. Chem.* **2017**, *8*, 97.
- 6 G. L. Semenza, *Nat. Rev. Cancer* **2003**, *3*, 721.
- 7 A. L. Harris, *Nat. Rev. Cancer* **2002**, *2*, 38.
- 8 J. M. Brown, W. R. William, *Nat. Rev. Cancer* **2004**, *4*, 437.
- 9 M. Takasawa, R. R. Moustafa, J. C. Baron, *Stroke* **2008**, *39*, 1629.
- 10 J. H. Crawford, T. S. Isbell, Z. Huang, S. Shiva, B. K. Chacko, A. N. Schechter, V. M. Darley-Usmar, J. D. Kerby, J. D. Lang, D. Hypoxia Kraus, *Blood* **2006**, *107*, 566.
- 11 C. Murdoch, M. Muthana, C. E. Lewis, *J. Immunol.* **2005**, *175*, 6257.
- 12 H. K. Eltzschig, D. L. Bratton, S. P. Colgan, *Nat. Rev. Drug Discov.* **2014**, *13*, 852.
- 13 X. Zheng, X. Wang, H. Mao, W. Wu, B. Liu, X. Jiang, *Nat. Commun.* **2015**, *6*, 5834.
- 14 W. R. Wilson, M. P. Hay, *Nat. Rev. Cancer* **2011**, *11*, 393.
- 15 S. Y. Sharp, L. R. Kelland, M. R. Valenti, L. A. Brunton, S. Hobbs, P. Workman, *Mol. Pharmacol.* **2000**, *58*, 1146.
- 16 K. Kiyose, K. Hanaoka, D. Oshiki, T. Nakamura, M. Kajimura, M. Suematsu, H. Nishimatsu, T. Yamane, T. Terai, Y. Hirata, T. Nagano, *J. Am. Chem. Soc.* **2010**, *132*, 15846.
- 17 W. Zhang, W. Fan, Z. Zhou, J. Garrison, *ACS Med. Chem. Lett.* **2017**, *8*, 1269.
- 18 M. P. Hay, W. R. Wilson, W. A. Denny, *Bioorg. Med. Chem.* **2005**, *13*, 4043.
- 19 Y. Ikeda, H. Hisano, Y. Nishikawa, Y. Nagasaki, *Mol. Pharm.* **2016**, *13*, 2283.
- 20 A. Chevalier, Y. Zhang, O. M. Khdour, J. B. Kaye, S. M. Hecht, *J. Am. Chem. Soc.* **2016**, *138*, 12009.
- 21 W. Piao, S. Tsuda, Y. Tanaka, S. Maeda, F. Liu, S. Takahashi, Y. Kushida, T. Ueno, T. Komatsu, T. Terai, T. Nakazawa, M. Uchiyama, K. Morokuma, T. Nagano, K. Hanaoka, *Angew. Chem. Int. Ed.* **2013**, *52*, 13028.
- 22 O. Kensuke, A. Chiho, H. Takashi, M. Masataka, M. Tadahiko, *Bioconjug. Chem.* **2012**, *23*, 324.
- 23 H. Cho, J. Bae, V. K. Garripelli, J. M. Anderson, H. W. Jun, S. Jo, *Chem. Commun.* **2012**, *48*, 6043.
- 24 H. Mutlu, C. M. Geiselhart, C. B. Kowollik, *Mater. Horiz.* **2018**, *5*, 162.
- 25 J. Y. Rao, A. Khan, *J. Am. Chem. Soc.* **2013**, *135*, 14056.
- 26 J. Y. Rao, C. Hottinger, A. Khan, *J. Am. Chem. Soc.* **2014**, *136*, 5872.
- 27 J. Y. Rao, A. Khan, *Polym. Chem.* **2015**, *6*, 686.
- 28 T. Eom, W. Yoo, Y. D. Lee, J. H. Park, Y. Choe, J. Bang, S. Kim, A. Khan, *J. Mater. Chem. B* **2017**, *5*, 4574.
- 29 T. Eoma, W. Yoo, S. Kim, A. Khan, *Biomaterials* **2018**, *185*, 333.
- 30 F. Perche, S. Biswas, T. Wang, L. Zhu, V. P. Torchilin, *Angew. Chem. Int. Ed.* **2014**, *53*, 3362.
- 31 P. Kulkarni, M. K. Haldar, S. You, Y. Choi, S. Mallik, *Bio-macromolecules* **2016**, *17*, 2507.
- 32 T. Thambi, V. G. Deepagan, H. Y. Yoon, H. S. Han, S. -H. Kim, S. Son, D. -G. Ahn, C. -H. Jo, Y. D. Suh, K. Kim, I. C. Kwon, D. S. Lee, J. H. Park, *Biomaterials* **2014**, *35*, 1735.

- 33** G. M. Anlezark, R. G. Melton, R. F. Sherwood, B. Coles, F. Friedlos, R. J. Knox, *Biochem. Pharmacol.* **1992**, *44*, 2289.
- 34** L. Hu, C. Yu, Y. Jiang, J. Han, Z. Li, P. Browne, P. R. Race, R. J. Knox, P. F. Searle, E. I. Hyde, *J. Med. Chem.* **2003**, *46*, 4818.
- 35** G. Xu, H. L. McLeod, *Clin. Cancer Res.* **2001**, *7*, 3314.
- 36** W. A. Denny, *Lancet Oncol.* **2000**, *1*, 25.
- 37** W. A. Denny, *Eur. J. Med. Chem.* **2001**, *36*, 577.
- 38** B. Prasai, W. C. Silvers, R. L. McCarley, *Anal. Chem.* **2015**, *87*, 6411.
- 39** L. Cui, Y. Zhong, W. Zhu, Y. Xu, Q. Du, X. Wang, X. Qian, Y. Xiao, *Org. Lett.* **2011**, *13*, 928.
- 40** T. Thambi, S. Son, D. S. Lee, J. H. Park, *Acta Biomater.* **2016**, *29*, 261.
- 41** C. H. Whang, K. S. Kim, J. Bae, J. Chen, H. W. Jun, S. Jo, *Macromol. Rapid Commun.* **2017**, *38*, 1700395.
- 42** R. Narain, S. P. Armes, *Biomacromolecules* **2003**, *4*, 1746.
- 43** J. Z. Du, S. P. Armes, *J. Am. Chem. Soc.* **2005**, *127*, 12800.
- 44** S. Y. Liu, S. P. Armes, *J. Am. Chem. Soc.* **2001**, *123*, 9910.
- 45** X. Z. Jiang, Z. S. Ge, J. Xu, H. Liu, S. Y. Liu, *Biomacromolecules* **2007**, *8*, 3184.
- 46** H. Liu, X. Z. Jiang, J. Fan, G. H. Wang, S. Y. Liu, *Macromolecules* **2007**, *40*, 9074.
- 47** C. H. Li, T. Wu, C. Y. Hong, G. Q. Zhang, S. Y. Liu, *Angew. Chem. Int. Ed.* **2012**, *51*, 455.
- 48** Z. Y. Deng, Y. F. Qian, Y. Q. Yu, G. H. Liu, J. M. Hu, G. Y. Zhang, S. Y. Liu, *J. Am. Chem. Soc.* **2016**, *138*, 10452.
- 49** Y. M. Li, G. H. Liu, X. R. Wang, J. M. Hu, S. Y. Liu, *Angew. Chem. Int. Ed.* **2016**, *55*, 1760.
- 50** Z. Q. Sun, G. H. Liu, J. M. Hu, S. Y. Liu, *Biomacromolecules* **2018**, *19*, 2071.
- 51** M. Ikeda, T. Tanida, T. Yoshii, I. Hamachi, *Adv. Mater.* **2011**, *23*, 2819.
- 52** S. Kumar, S. G. Roy, P. De, *Polym. Chem.* **2012**, *3*, 1239.
- 53** J. Hu, C. Li, S. Liu, *Langmuir* **2010**, *26*, 724.
- 54** Y. Li, Y. Sun, J. Li, Q. Su, W. Yuan, Y. Dai, C. Han, Q. Wang, W. Feng, F. Li, *J. Am. Chem. Soc.* **2015**, *137*, 6407.
- 55** Z. Zhang, K. Tanabe, H. Hatta, S. I. Nishimoto, *Org. Biomol. Chem.* **2005**, *3*, 1905.
- 56** M. Wilhelm, C. L. Zhao, Y. Wang, R. Xu, M. A. Winnik, J. L. Mura, G. Riess, M. D. Croucher, *Macromolecules* **1991**, *24*, 1033.
- 57** D. J. Adams, D. Atkins, A. I. Cooper, S. Fuzeland, A. Trewin, I. Young, *Biomacromolecules* **2008**, *9*, 2997.
- 58** A. Blanazs, S. P. Armes, A. J. Ryan, *Macromol. Rapid Commun.* **2009**, *30*, 267.
- 59** A. Alouane, R. Labruère, T. L. Saux, F. Schmidt, L. Jullien, *Angew. Chem. Int. Ed.* **2015**, *54*, 7492.